International Journal of Pharmaceutics 369 (2009) 162–169

Contents lists available at ScienceDirect

International Journal of Pharmaceutics

journal homepage: www.elsevier.com/locate/ijpharm

Pharmaceutical Nanotechnology

# The effect of the structure of small cationic peptides on the characteristics of peptide-DNA complexes

Geetha N. Goparaju[a], C. Satishchandran[b], Pardeep K. Gupta[a,*]

[a] The University of the Sciences in Philadelphia, 600 South 43rd Street, Philadelphia, PA 19104, USA
[b] Institute for Hepatitis & Virus Research, Doylestown, PA 18902, USA

ARTICLE INFO

*Article history:*
Received 10 August 2008
Accepted 21 October 2008
Available online 7 November 2008

*Keywords:*
Non-viral gene delivery
Cationic amphiphilic peptides
Particle size
Zeta potential

ABSTRACT

A series of transcriptional activator (TAT)–protein transduction domains (PTDs) modified with hydrophobic amino acids were used as model cationic amphiphilic peptides to study the effect of hydrophobicity on interaction of such peptides with plasmid DNA. The peptide–DNA complexes were analyzed by dynamic light scattering and gel electrophoresis to determine their size and electrokinetic properties at various +/− charge ratios. Peptides in solution were found to have a tendency to aggregate and the hydrodynamic size of the aggregates depends on the structure of peptide. Peptides with smaller hydrophobic residues at the N-terminal formed smaller complexes with DNA compared to the ones with larger hydrophobic tails. DNA complexes having peptides with more than one hydrophobic moiety at the N-terminal had a tendency to aggregate. Among the peptides having single hydrophobic amino acid at the N-terminal, DNA complexes of Tyr-TAT and Phe-TAT were found to be stable in solution. The size of the hydrophobic domain and the type of hydrophobic amino acid at the N-terminal of cationic amphiphilic peptides play an important role not only in the complex formation but also in stabilizing the system. The studies presented here indicate that there is a potential for strategic development of these peptides into potential non-viral gene delivery vectors.



## 1. Introduction

Considering the significant importance gained by cationic amphiphilic peptides as non-viral vectors for gene delivery, there is a need for a better understanding of their interaction with DNA for improving their efficiency. The size and surface charge of the cationic peptide–DNA complexes not only influence their colloidal stability in vitro but also their stability in vivo and subsequently their efficiency. Therefore, it is very important to understand how structural features of the cationic peptide influence these properties.

Interaction of peptides with DNA involves both electrostatic and hydrophobic interactions. Electrostatic interactions come from phosphate groups on DNA and amino groups of the peptides. The importance of the hydrophobic components becomes apparent upon consideration of the DNA duplex. Though dominated by the phosphate groups within the backbone, this structure also displays several non-polar regions. One strategy in the design of DNA-binding molecules is to occupy these regions with complementary hydrophobic bulk, excluding water from this interface. The resultant favorable binding to these regions, including the C5, C6 of pyrimidine, 5-methyl group of the thymine, C2′, C5′ and other atoms from the sugar ring found in the groove walls and the space between the base pairs of DNA are the available hydrophobic regions on DNA. Hydrophobic side chains of amino acids can make hydrophobic contacts with one of the hydrophobic sites on DNA, thus stabilizing the complex. Three types of interaction account for selective molecular recognition and binding between DNA and proteins in biological systems. These are (i) shape specific interactions between aromatic side chains, such as the indole moiety of Trp or the aromatic side chains of Phe and Tyr, and DNA bases; (ii) hydrogen bonding interactions between hydrophilic side chains (Tyr, Asn, Ser, Thr, and His) and nucleotides; (iii) ionic interactions involving positively charged side chains (Arg, Lys, and His) and the phosphodiester backbone of DNA (Keller et al., 2002). There are at least two types of hydrophobic forces that have been experimentally verified for small molecule–DNA interactions. They are (i) intercalation of planar aromatic residues between base pairs of DNA and (ii) external hydrophobic type binding of large "hydrophobic" cations, like steroidal amines (Gabbay and Kleinman, 1970). The intercalation of the aromatic amino groups needs lot of energy and bending of the molecule. In recent times, many models have been proposed for interaction of oligopeptides with DNA. According to the model of complimentary interaction between ds DNA and small peptides,

* Corresponding author.
*E-mail address:* p.gupta@usip.edu (P.K. Gupta).

0378-5173/$ – see front matter © 2008 Elsevier B.V. All rights reserved.
doi:10.1016/j.ijpharm.2008.10.028

polar interactions between the peptide and base pairs in the double helix are determined by electrostatic interactions of peptide carboxyl groups with amino groups of adenine and cytosine, by hydrogen bonds of proton-carrying amino groups and carboxyl groups of the peptide with nitrogen atom 7N of adenine and guanine. Hydrophobic interactions in the system are determined by lateral groups of the peptide and methyl groups of thymine (Malinin and Khavinson, 2005).

Considering the above factors, it becomes apparent that the structural features of the peptide influence their complex formation with DNA. Binding of polycations was found to induce DNA compaction due to compensation of electrostatic charges of DNA and hydrophobic interactions of the complexed sites (Kabanov and Kabanov, 1995). Apart from the clustering of polycations, other structural elements like hydrophobicity of the polycation and spatial arrangement of the charges is also important. Yoshikawa et al. worked with diaminoalkanes [$(NH_3{}^+9CH_2)_n$ $NH_3{}^+$, where $n = 1–6$] for condensation and concluded that when $n = 3$ and 5, DNA was condensed and there was no condensation when $n = 2$, 4 and 6 (Yoshikawa and Yoshikawa, 1995). Niidome et al. showed that cationic peptides containing three or six repeats of tetra peptide units Leu-Ala-Arg-Leu were observed to bind and condense DNA, but the binding was significantly reduced when some of the leucines were substituted by serines (Niidome et al., 1997). Gottschalk et al. showed that condensation of DNA improved when tryptophan (Tryp) was present in the peptide (Gottschalk et al., 1996). It was suggested that the improved condensation might be due to the increase in hydrophobicity of the peptide or possibly a more specific role of tryptophan in intercalating into DNA to provide a more ordered condensation. The nature of uncharged and basic amino acids, the length of fatty acid chains covalently attached to the peptide and carboxy-terminal modifications have also been shown to have a significant influence on DNA binding and gene transfer efficiency (Smith et al., 1998; Mahato et al., 1999; Blessing et al., 1998; Wadhwa et al., 1997). Therefore, it is important to understand how the hydrophobic sites in cationic peptides influence the interaction with DNA and as a result affect the properties of these complexes as applicable to gene delivery.

In this study, for the purpose of developing novel amphiphilic peptides with a short chain length as non-viral vectors for gene delivery, and to understand the effect of the hydrophobic N-terminal on interaction of the peptides with DNA; we designed and synthesized peptides based on transcriptional activator (TAT)–protein transduction domains (PTDs) by sequentially modifying the N-terminal. TAT–PTD is a member of proteins called protein transduction domains or cell-penetrating peptides (CPPs) useful for intracellular delivery of various cargoes with molecular weights several times greater than their own (Chakrabarti et al., 1989). This process of protein transduction was discovered first by Green and Frankel independently; who found that 86-mer trans-activating transcriptional activator from HIV-1 was efficiently taken up by various cells, when added to the surrounding media (Arnheiter and Haller, 1988; Straubinger et al., 1985). The protein transduction sequence for TAT includes residues 47–57 (11-mer; Tyr-Gly-Arg-Lys-Lys-Arg-Arg-Gln-Arg-Arg-Arg) (Schwarze et al., 2000). While investigating the role of arginine rich motifs in gene delivery, it was demonstrated that the oligomers of TAT–PTD compacted plasmid DNA to nanometric particles and stabilized DNA toward nuclease degradation. Such TAT peptide complexes were superior to standard polyethyleneimine vectors in terms of transfection efficiency. In addition, gene transfer was enhanced due to TAT nuclear localization sequence (Rudolph et al., 2003). TAT–PTD interacted with plasmid DNA electrostatically and the resulting complexes were transferred to mammalian cells by the endocytosis-mediated pathway (Ignatovich et al., 2003). In the present study we used TAT–PTD and modified TAT–PTDs as model cationic amphiphilic peptides. The N-terminal of TAT–PTD was systematically varied with hydrophobic amino acids in order to understand the influence of the hydrophobic N-terminal of cationic amphiphilic peptides on size and electrokinetic properties of complexes with DNA.

The primary goal of this study is to evaluate the influence of the hydrophobic N-terminal of the cationic peptides on the size and the electrokinetic properties of the DNA–peptide complexes. Studies of this type, not only help in identifying the physical characteristics that are beneficial for non-viral vectors but also for identifying the factors that influence the stability of the complexes in vitro.

## 2. Materials and methods

### 2.1. Materials

TAT–PTD and other modified peptides were synthesized in our laboratory by solid phase peptide synthesis (SPPS). TAT–PTD was modified to obtain additional peptides containing different residues of tyrosine (Tyr), phenylalanine (Phe), valine (Val), leucine (Leu) and tryptophan (Tryp) at the N-terminal. Plasmid DNA, gWiz GFP (5.75 kbp) encoding green fluorescent protein (GFP), was generously provided by Nucleonics Inc. All the other materials such as sodium phosphate, sodium hydroxide, N,N′diisopropylcarbodiimide (DIC), 1-hydroxybenzotriazole hydrate (HOBT), piperidine, dichloromethane (DCM), methanol, hexane, trifloroacetic acid (TFA), thianisole, dimethylformamide (DMF), and ether were obtained and were used as provided by Fisher Scientific Co. (Fair Lawn, NJ) or Sigma Chemical Co. (St. Louis, MO). Fmoc-Tyr, Fmoc-Phe, Fmoc-Gly, Fmoc-Arg, Fmoc-Gln and Wang resin were purchased from American Peptide Company (Sunnyvale, CA).

### 2.2. Peptide synthesis

All the peptides were synthesized by solid phase peptide synthesis. Initially Arg-wang resin was wetted and was kept for swelling with dichloromethane. It was further washed with DCM. The arginine was deprotected with 20% piperidine solution in dimethylformamide. The weighed quantity of appropriate Fmoc amino acid was activated using HOBt and DIC. The activated amino acids were then added to the deprotected resin and stirred for 1.5 h. Following the reaction, the peptide solution was drained and washed five times with DMF. After this step, the final peptide was recovered or the next amino acid was added after deprotection. The resin were washed with DMF, DCM, methanol and hexane and dried after completion of each peptide. The peptides from the dry resins were cleaved by adding the cleavage reagent TFA/TIS/water (95 ml/2.5 ml/2.5 ml) and were left stirring for 2 h. The peptides were collected and further purified by adding cold ether and their purity was analyzed by reverse phase (RP)-HPLC.

### 2.3. Preparation of pDNA–peptide complexes

All peptides and pDNA solutions were dialyzed against 10 mM phosphate buffer of pH 7.4 overnight using a dialysis membranes of MWCO 500 and 3500, respectively. Different proportions of 1 mg/ml of pDNA solution and peptides were mixed to get peptide–DNA complexes at the desired +/− ratios. Here +/− ratio indicates the ratio of number of positive charges from amino groups of peptides to the number of negative charges from phosphate groups of DNA The complexes were kept at room temperature

before transferring to the gel for electrophoresis or for size and zeta potential analysis.

### 2.4. Gel electrophoresis

The extent of DNA charge neutralization by TAT–PTD and modified TAT–PTDs was studied by estimating the mobility of the complexes in a 0.75% (w/v) agarose gel using 0.5× TBE buffer. The peptide–DNA complexes were analyzed at different +/− ratios in a horizontal gel electrophoresis unit for 1.5 h at 90 V. The gel was immersed in ethidium bromide solution of concentration 0.5 μg/ml for 30–45 min after completion of electrophoresis. The gel was then immersed in water for 20 min to remove the excess ethidium bromide. A UVA Image station was used to digitally image the gel.

### 2.5. Size and zeta potential analysis

The size and zeta potential of the complexes as a function of +/− ratio were analyzed by dynamic light scattering (DLS) using MALVERN Zeta Sizer Nano. The instrument was initially validated using the standards for size and zeta potential provided by the manufacturer. Standard of 60 nm for size and −15 mV for zeta potential were used for validation. All the measurements were performed in 10 mM phosphate buffer with pH 7.4. The final pDNA concentration was maintained at 50 μg/ml for all the measurements. The size and zeta potential of pDNA alone were also determined. Refractive index for these measurements was set at 1.335. Polydispersity index (PDI) of the samples was also estimated during size analysis. The size data from cumulant analysis and volume distribution has been compared to make final conclusions about size. Z-average diameter for peptide–DNA complexes has been reported in this study. The zeta potential was measured from the electrophoretic mobility of the samples. All the data has been expressed as mean ± standard deviation.

## 3. Results and discussion

### 3.1. Design of peptides

All the peptides used in the study were synthesized by solid phase peptide synthesis using F-moc chemistry. The purity of the synthesized peptide derivatives was determined by reversed phase-HPLC and all the peptides have purity over 98%. The peptide sequence used in the study for TAT is the amino acid sequence of the protein transduction domain pertaining to 47–57 aminoacids of TAT protein. TAT–PTD was sequentially modified at the N-terminal to have varying hydrophobicity. TAT–PTD has glycine (Gly), lysine (Lys), arginine (Arg), glutamine (Glu) and tyrosine (Tyr). Due to its small size, glycine imparts flexibility to any protein/peptide. Arginine and lysine contribute towards the cationic charges. Hydrophobic amino acids tyrosine and phenylalanine were added to have 1, 3, or 5 hydrophobic residues at the N-terminal of TAT–PTD. Attaching neutral hydrophobic amino acids will preserve the existing high positive charge present in TAT–PTD and at the same time increases the hydrophobicity of these derivatives. Later on, during the course of the study additional peptides with one leucine or valine or tryptophan were synthesized for further evaluation. The primary structure, molecular weight, and number of charges on the peptides are shown in Table 1. Hydrophobicity of these peptides increases with increasing number of hydrophobic amino acids at the N-terminal. Valine, leucine and phenylalanine are more hydrophobic than tyrosine and tryptophan (Table 4). Tyrosine, tryptophan and phenylalanine are aromatic in nature. Based upon the hydrophobic nature of the attached amino acids, the peptides can be arranged in increasing order of hydrophobicity as shown below:

$$\text{TAT} < \text{Tyr-TAT} < \text{Tryp-TAT} < \text{Phe-TAT} < \text{Leu-TAT} < \text{Val-TAT} < \text{Tyr}_3\text{-TAT} < \text{Tyr}_5\text{-TAT} < \text{Phe}_3\text{-TAT} < \text{Phe}_5\text{-TAT}$$

**Table 1**
List of peptides used in the study.

| Peptides | Amino acid sequence | Molecular weight | Number of charges |
|---|---|---|---|
| I TAT | Tyr-Gly-Arg-Lys-Lys-Arg-Arg-Gln-Arg-Arg-Arg | 1558 | +8 |
| II | Tyr-TAT | 1721 | +8 |
| III | $Tyr_3$-TAT | 2047 | +8 |
| IV | $Tyr_5$-TAT | 2862 | +8 |
| V | Phe-TAT | 1705 | +8 |
| VI | $Phe_3$-TAT | 1999 | +8 |
| VII | $Phe_5$-TAT | 2293 | +8 |
| VIII | Leu-TAT | 1672 | +8 |
| IX | Val-TAT | 1657 | +8 |
| X | Tryp-TAT | 1744 | +8 |

### 3.2. Size analysis of peptides

As seen in Table 2, the hydrodynamic diameter of TAT, Phe-TAT, Leu-TAT, Val-TAT, and Tryp-TAT is very low ranging from 1.97 to 2.47. The hydrodynamic diameter is 305.9 nm for Tyr-TAT. It can be seen that peptides with tyrosine form larger aggregates compared to peptides containing phenylalanine. The data represented here corresponds to the volume distribution of size analysis obtained from dynamic light scattering. The polydispersity index of the peptides was found to be below 0.4. Size analysis of 1 mg/ml peptide solution in water by dynamic light scattering indicates aggregation behavior for some peptides. The peptides used in this study are small with their molecular weight ranging approximately from 1500 to 2800 (Table 1). Size analysis data indicates aggregate formations which contain monomers as low as 2 to as high as 100 or 150 depending on the type of peptide. The simultaneous presence of distinct interactions (e.g., hydrogen bonding, electrostatic, and hydrophobic interactions) in the system leads to rich and subtle molecular self-assembly behavior. It is understood that the aggregation of peptides is a result of subtle interplay between various intra- and inter-chain interactions, i.e., interactions within a single chain and interaction between different chains, respectively. The presence of aromatic residues is thought to be important to stabilize the aggregate to form critical aggregation nucleus which is the first step towards further growth of the aggregate (Gsponer et al., 2003). The stability of the formed aggregates depends on the type of hydrophobic residue, the concentration being a key parameter in controlling the self-assembly of the peptides (Fung et al., 2003; Peggion et al., 1970; Sjögren et al., 2005; Sjögren and Ulvenlunda, 2005). The presence of the same hydrophobic amino acids (tyrosine pep-

**Table 2**
Size of the peptides in solution as measured by dynamic light scattering.

| Peptide | Size from volume distribution (nm) |
|---|---|
| TAT | 2.0 ± 0.4 |
| Tyr-TAT | 305.9 ± 44.2 |
| $Tyr_3$-TAT | 159.1 ± 27.3 |
| $Tyr_5$-TAT | 296.8 ± 36.4 |
| Phe-TAT | 1.6 ± 0.2 |
| $Phe_3$-TAT | 119.5 ± 2.3 |
| $Phe_5$-TAT | 156.2 ± 3.3 |
| Leuc-TAT | 2.1 ± 0.3 |
| Val-TAT | 2.5 ± 0.6 |
| Tryp-TAT | 2.0 ± 0.2 |

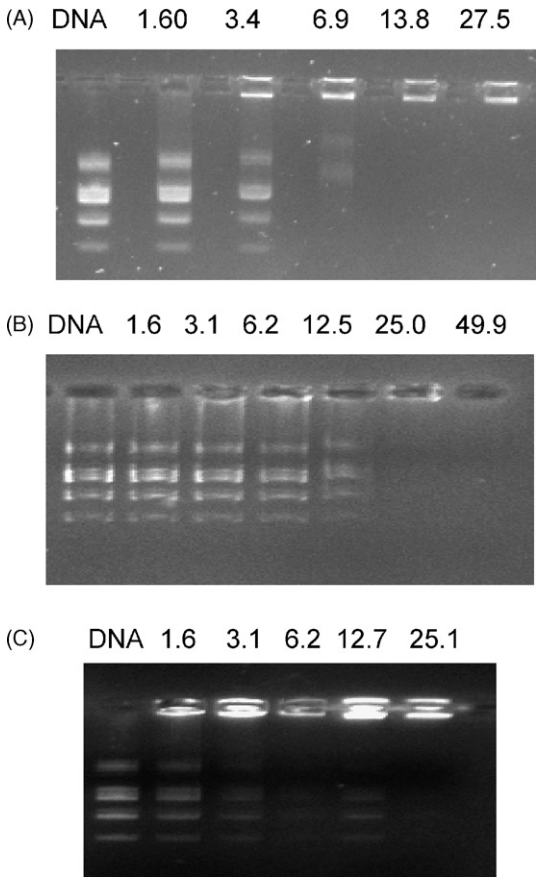


**Fig. 1.** Gel electrophoresis of peptide–DNA complexes. The values shown on the figures are +/− ratios of the complexes. The left most lane in each figure indicates the mobility of DNA alone in the gel. Subsequent lanes from left to right indicate mobility of DNA in the presence of peptide at various +/− ratios indicated above the lane. (A) TAT; (B) Tyr-TAT; (C) Phe-TAT.

tides) at the N-terminal resulted in formation of smaller aggregates when compared with the peptides having different hydrophobic amino acids (phenylalanine peptides). More in-depth studies would be required to establish, the type of aggregates formed for each peptide used in this study and their critical aggregation concentration.

### 3.3. Gel electrophoresis

Charge neutralization of DNA was examined by electrophoretic mobility of the peptide–DNA complexes in a 0.75% agarose gel. DNA was detected by staining with ethidium bromide. The gel electrophoresis pictures are shown in Fig. 1. In all the gels, DNA by itself indicates maximum migration. The mobility of DNA gradually decreases as we move from lower +/− ratios to higher ratios. This is because of increase in the extent of neutralization of charge on the DNA by increasing concentration of the peptides. For all the peptides except $Phe_3$-TAT, the DNA shows complete neutralization of charge between +/− ratios of 3.2 and 30. The optimal +/− ratios at which complete retention of DNA was observed are given in Table 3. For $Phe_3$-TAT, neutralization is indicated at +/− ratio of 78. This indicates a rather poor interaction of this peptide with DNA. Gel electrophoresis for Leu-TAT, Val-TAT and Tryp-TAT and DNA complexes was performed from lower +/− ratio of 0.4. These complexes showed precipitation at +/− ratio of 6.4. As the peptide concentration in the system increases, the charge on the DNA is neutralized. The surface charge of the complexes also increases gradually towards a less negative value because of charge neutralization of DNA. When the concentration of the peptide is enough to neutralize 90% of the charge on DNA, the DNA is condensed into compact particles. This can be clearly seen in the gel electrophoresis data (Fig. 1A–C and Table 2). The presence of different bands in the gel might be because of the presence of a small percent of linear and nicked DNA as well as partially condensed DNA in the sample. Electrophoretic mobility of the samples in the gel depends on various factors like the size, shape and surface charge of the complexes.

**Table 3**
Optimal +/− ratio where immobility of DNA was seen in gel electrophoresis.

| Peptide | +/− |
|---|---|
| $Tyr_3$-TAT | 21.0 |
| $Tyr_5$-TAT | 30.1 |
| $Phe_3$-TAT | 78.0 |
| $Phe_5$-TAT | 18.7 |
| Leuc-TAT | 6.4 |
| Val-TAT | 3.2 |
| Tryp-TAT | 3.2 |

#### 3.3.1. Size analysis of peptide–DNA complexes

The hydrodynamic size of native DNA was found to be 29.11 nm ± 5.7. Data from size analysis of peptide–DNA complexes is shown in Fig. 2A–C. Tyr-TAT and Phe-TAT result in much smaller complexes whose hydrodynamic size ranges between 78.15 to 102 nm, and 67–89 nm, respectively. The polyplexes produced by TAT have a hydrodynamic size ranging from 300 to 470 nm. The size of DNA complexes formed by $Tyr_3$-TAT shows lower size compared to TAT, which range from 108.4 to 310.5 nm. $Tyr_5$-TAT results in DNA complexes of maximum size ranging between 248.5 and 546.5 nm (Fig. 2A) compared to other tyrosine containing peptides. Among peptides containing phenylalanine, again $Phe_3$-TAT–DNA complexes are larger compared to TAT–DNA, Phe-TAT–DNA complexes. DNA complexes formed from $Phe_5$-TAT show a larger size initially up to +/− ratio of 5.0 and the size decreases thereafter (Fig. 2B). DNA complexes formed by Leu-TAT, Val-TAT and Tryp-TAT show a size range of 105.83–266 nm between +/− ratios of 0.4 and 3.2. DNA complexes formed from these peptides are unstable in solution above +/− ratio of ~6.0 as indicated by precipitation at higher +/− ratios.

#### 3.3.2. Polydispersity (PDI) of the peptide–DNA complexes

PDI is an indication of heterogeneity of the various size populations in the sample. The PDI of the complexes is given in Fig. 4A–C. The PDI of TAT–DNA complexes ranges from 0.35 to 0.54. It increases up to +/− ratio of 17.2 and decreases afterwards. PDI of Tyr-TAT–DNA complexes are almost constant throughout +/− charge ratios studied and ranges between 0.28 and 0.35. Tyr3-TAT–DNA and Tyr5-TAT–DNA complexes indicate a PDI ranging between 0.25 and 0.42 (Fig. 4A). PDI of $Phe_{1,3,5}$-TAT peptides ranges between 0.3

**Table 4**
Hydrophobicity values of hydrophobic amino acids used in the study.

| Amino acid | Hydrophobic index (kcal/mol)[a] |
|---|---|
| Tryptophan | −0.9 |
| Tyrosine | −1.3 |
| Phenylalanine | 2.8 |
| Leucine | 3.8 |
| Valine | 4.2 |

[a] Kyte and Doolittle scale of amino acid hydrophobicity (Kyte and Doolittle, 1982).

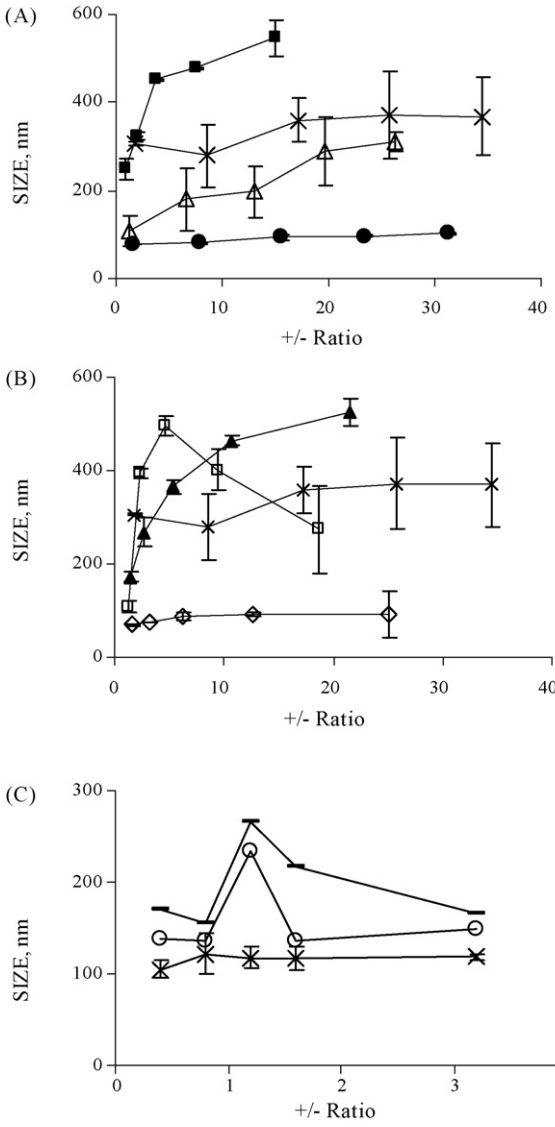


**Fig. 2.** Particle size (z-average diameter) of peptide-complexes at various +/− ratios as analyzed by dynamic light scattering. Values expressed as mean ± S.D., $n = 3$. Standard deviations in (C) are not indicated to maintain clarity of the graph. Standard deviations ranged from 2.3 to 135.4. (A) [×] TAT, [●] Tyr-TAT, [△] $Tyr_3$-TAT, and [■] $Tyr_5$-TAT. (B) [×] TAT, [◊] Phe-TAT, [▲] $Phe_3$-TAT, and [□] $Phe_5$-TAT. (C) [–] Leu-TAT, [×] Val-TAT, and [○] Tryp-TAT.

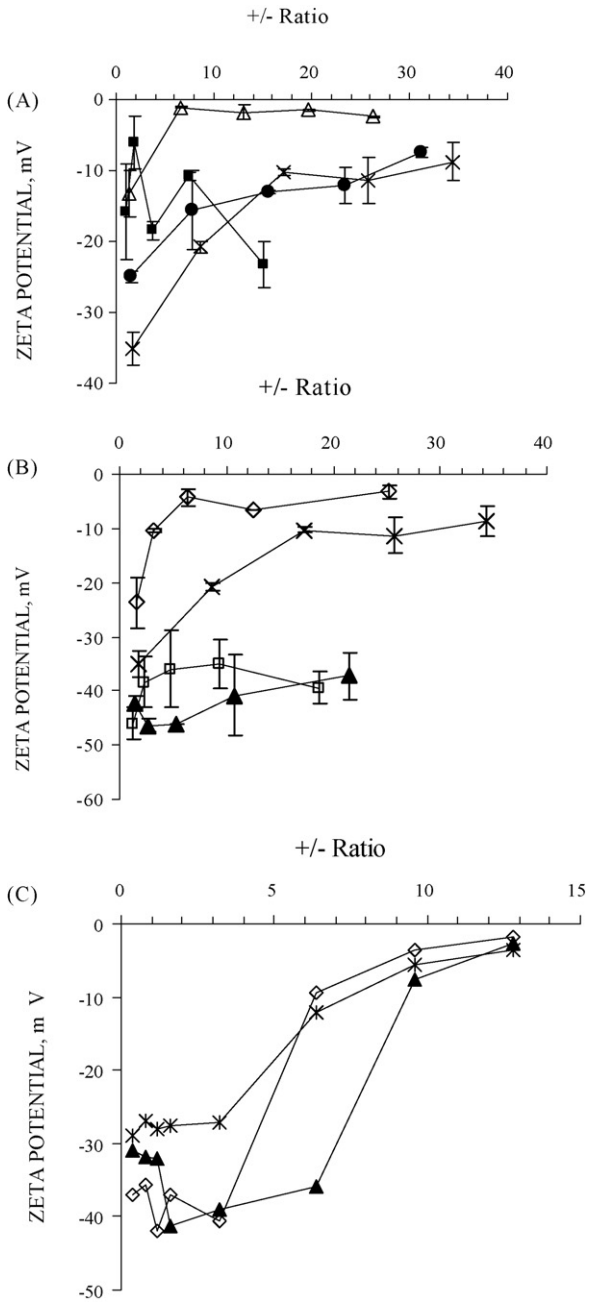


**Fig. 3.** Zeta potential of peptide-complexes in 10 mM phosphate buffer, pH 7.4 at various +/− ratios. Values expressed as mean ± S.D., $n = 3$. Standard deviations in (C) have not been indicated to maintain the clarity of the graph. S.D. ranged from 1.32 to 13.5. (A) [×] TAT, [●] Tyr-TAT, [△] $Tyr_3$-TAT, and [■] $Tyr_5$-TAT. (B) [×] TAT, [◊] Phe-TAT, [▲] $Phe_3$-TAT, and [□] $Phe_5$-TAT. (C) [–] Leu-TAT, [×] Val-TAT, and [○] Tryp-TAT.

and 0.54 (Fig. 4B). The PDI of Leu, Val, Tryp-TAT–DNA complexes ranges from 0.4 to 0.7. The high PDI of the complexes at +/− of 1.6 is an indication of aggregation at charge neutralization of complexes further leading to precipitation (Fig. 4C).

### 3.3.3. *Zeta potential analysis of peptide–DNA complexes*

The zeta potential of DNA was found to be −52.3 mV ± 1.7. The change in zeta potential of DNA complexes formed by TAT peptides containing tyrosine, indicate that the surface charge of the DNA is increased upon interaction with the peptides (Fig. 3A–C). As the concentration of the peptide increases, the net zeta potential becomes less negative from −52.3 mV, indicating interaction of the peptides with DNA. DNA complexes of TAT and Tyr-TAT show a similar change in net zeta potential. DNA-$Tyr_3$-TAT complexes show a higher net zeta potential compared to the other complexes at all +/− ratios and it almost remains constant after +/−6.5 (Fig. 3A). $Tyr_5$-TAT and DNA complexes though initially show an increase in zeta potential; there is a gradual decrease after +/− 2.0. Among the peptides containing phenylalanine, Phe-TAT indicates DNA complexes with higher surface charge followed by TAT. DNA complexes of $Phe_3$-TAT and $Phe_5$-TAT show very low change in zeta potential with increase in peptide concentration, even at very high N/P ratios (Fig. 3B). DNA complexes of Leu-TAT, Val-TAT and Tryp-TAT show similar change in zeta potential (Fig. 3C). Moreover, the zeta potential reported here is a reflection of the concentration at which the samples were prepared, the solution parameters such as ionic strength, the buffer species, etc. These values will change when the conditions mentioned change.

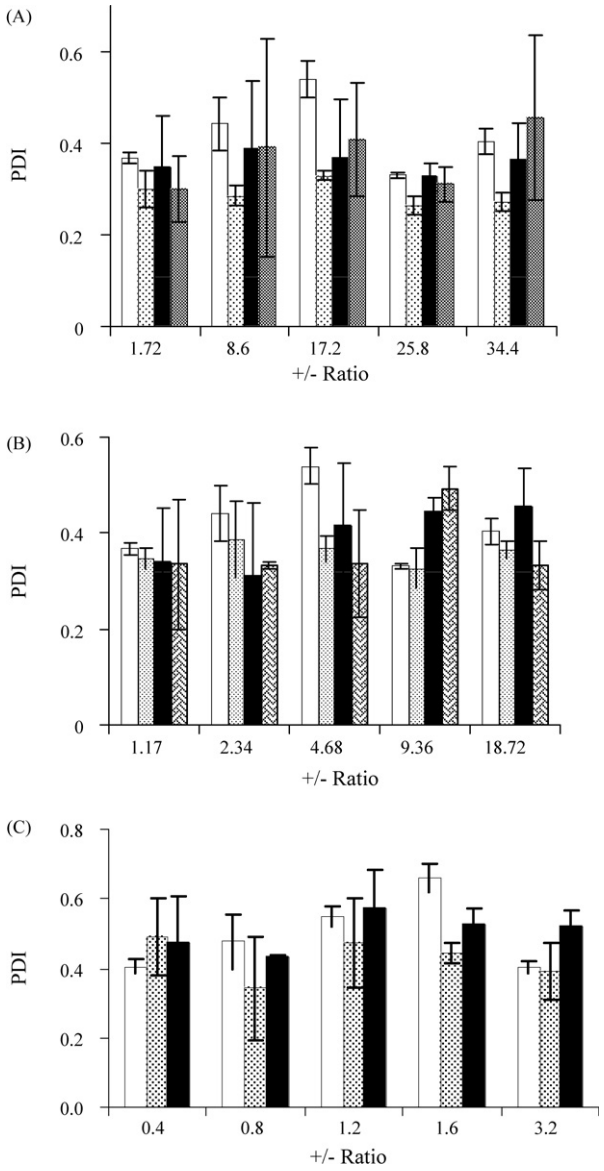


**Fig. 4.** Polydispersity index (PDI) of peptide-complexes at various +/− ratios. Values expressed as mean ± S.D., $n = 3$. (A) [□] TAT, [▨] Tyr-TAT, [■] $Tyr_3$-TAT, and [▩] $Tyr_5$-TAT. (B) [□] TAT, [▨] Phe-TAT, [■] $Phe_3$-TAT, and [▩] $Phe_5$-TAT. (C) [□] Leu-TAT, [▨] Val-TAT, and [■] Tryp-TAT.

### 3.4. Final discussion

A closer observation of the hydrodynamic size of the polyplexes indicates that Tyr-TAT and Phe-TAT peptides show smaller complexes compared to TAT (Fig. 2). The size of complexes formed by TAT correlates to the hydrodynamic size of the polyplexes formed by using cysteine flanked TAT at both the ends (Cys-TAT-Cys) in a study done by Manickam et al. (2005). There are two important features of Tyr-TAT and Phe-TAT interaction with DNA. First, these peptides are able to efficiently condense DNA into smaller particles than any other peptides; secondly they are able to stabilize the system without further aggregation within +/− ratios studied. The polydispersity index of the formed complexes is also low compared to other peptide–DNA complexes (Fig. 4A–C). The mixing of nucleic acid and polycation aqueous solutions results in binding of electrostatically complimentary chains. When the polycation has a hydrophobic domain, it sticks to the nucleic acid because it has to hide from the surrounding aqueous environment (Kabanov and Kabanov, 1995). When this hydrophobic site is small such as tyrosine or phenylalanine (Tyr-TAT and Phe-TAT), it can interact with the hydrophobic areas of the DNA and when 90% or more of the charge on DNA is neutralized, the DNA condenses into a tightly packed structured particle. This might be the case with Tyr-TAT and Phe-TAT. This model for interaction is depicted in Fig. 5. However, it is important to note here that the N-terminal of TAT also has one tyrosine, which means we are looking at two tyrosines in Tyr-TAT, and tyrosine and phenylalanine in Phe-TAT. It has been shown previously that condensation of DNA strongly depends on the structure of the polycation. A study done on collapse of DNA using isovalent polyamines spermine and a series of its homologues, $H_2N(CH_2)_3NH(CH_2)_{n=2-12}NH{-}(CH_2)_3NH_2$ ($n = 4$ for spermine) indicated formation of compact particles of hydrodynamic radius ($R_h$) of 40–50 nm for compounds with $n = 3$–6. The hydrodynamic radius increased further with increase in methylene chain length separating amino groups of the polyamines ($R_h = 60$–70 nm for $n = 7$–10 and >100 nm for $n = 11$ and 12) (Vijayanathan et al., 2001).

Stability of the size of polyplexes formed by Tyr-TAT and Phe-TAT at higher +/− ratios could be explained by considering the structure of the peptides (Fig. 2A). The size and zeta potential for these complexes has been studied from +/− ratio of 1.7–30 approximately. The size of these complexes is fairly constant within the +/− ratios studies. This indicates that the polyplexes formed by Tyr-TAT and Phe-TAT are stable in the presence of excess cationic peptide. From the peptide size analysis, aggregation of the peptides is clearly seen at a concentration of 1 mg/ml. The PDI of the formed complexes is also low compared to other peptide–DNA complexes (Fig. 4). Though the critical aggregation concentration of the peptides has not been determined, there is always a possibility of formation of aggregates of the excess free peptide in solution if the concentration of the free peptide reaches critical aggregate concentration. Whether the formed aggregates are small or large, they are able to stabilize the system by electrostatic repulsion because the hydrophobic domain of the peptide would be buried in the interior of the aggregate while the hydrophilic domain would extend out into solution. However, if the free peptide concentration does not reach critical aggregate concentration, then the free peptide can stabilize the polyplexes by a phenomenon which is similar to stabilization of DNA condensates by surfactants (Sharma et al., 2005). The hydrophilic charged domain of the peptide extends into water and sterically hinders the complexes from approaching each other while the small hydrophobic domain interacts with the polyplexes. Moreover, it is a proven fact that the excess cationic agent on the polyplexes is in equilibrium with the free cationic agent in the surrounding solution (Kabanov and Kabanov, 1995).

It was important to see if other TAT peptides containing single hydrophobic amino acid at the N-terminal would behave similarly. In order to look into this aspect, Leu-TAT, Val-TAT and Tryp-TAT were observed. One major difference between these peptides and Tyr-TAT and Phe-TAT peptides in that the polyplexes formed by these peptides precipitate at +/− ratio of approximately 6. Gel electrophoresis for these peptide–DNA complexes indicates decreasing mobility of DNA in the gel as we move from peptide: DNA +/− ratio of 0.4–3.2. There is clear band of DNA seen in the well at higher ratios. This might be because of precipitation of the complexes. Therefore, the size analysis was performed at +/− ranging from 0.4 to 3.2.

The size of the polyplexes formed with Leu-TAT, Val-TAT and Tryp-TAT indicate hydrodynamic sizes less than 300 nm and Val-TAT typically indicates polyplexes ranging between 105 and 118 nm (Fig. 2C). When the +/− ratio is close to 1, the size of the polyplexes increases for Leu-TAT and Tryp-TAT and upon further addition of the peptide, the size decreases and finally when more peptide is added

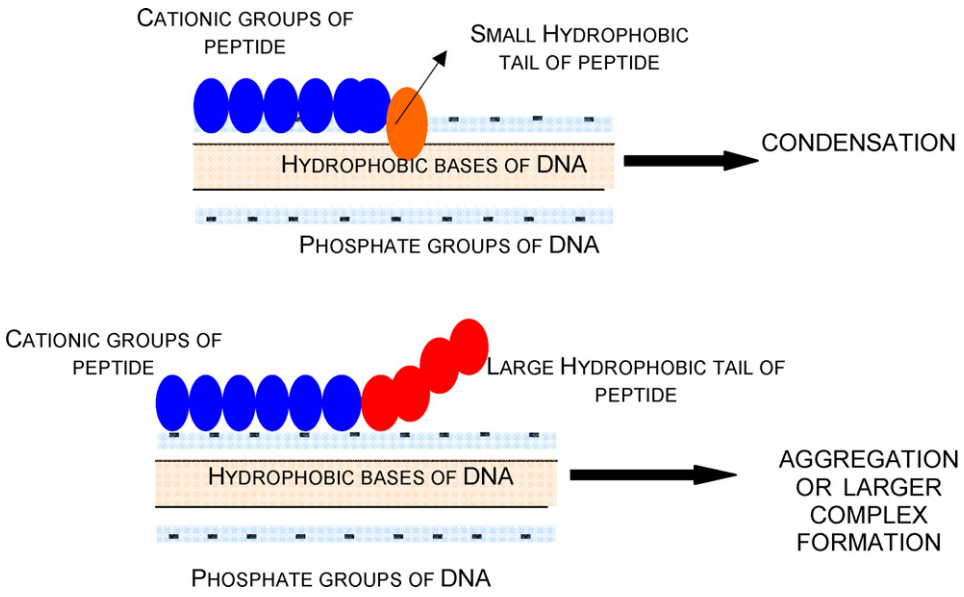


**Fig. 5.** Model for interaction of amphiphilic peptides with DNA.

the polyplexes precipitate out of solution for all the three peptides. This becomes more prominent at high +/− ratios. Isothermal titration calorimetry studies on these complexes indicate condensation of DNA close to +/− ratio of 3.2 for Leu-TAT and Val-TAT (data not shown here). This indicates that these peptides do condense DNA. However, the condensed particles are not stable in solution. They aggregate and finally precipitate out of solution. The aggregation of the complexes is also evident from the high polydispersity index of these complexes given in Fig. 4C. Aggregation might occur because of increased hydrophobicity of the complexes (Fig. 5). Out of all the amino acids used, valine and leucine are the most hydrophobic with hydrophobicity values of 3.8 and 4.2, respectively. They do not have an aromatic structure. They can interact with other hydrophobic areas on the DNA. This increases hydrophobic sites on the surface of the polyplexes as more and more peptide is added. At some point the complex reaches a critical composition and its hydrophobicity increases to such an extent that further binding of the polycation should lead to precipitation of the complex. When the zeta potential of the supernatant after precipitation (+/− of 4) is analyzed, we see a change in the zeta potential, indicating presence of some soluble complexes in solution (Kabanov et al., 1991; Miller and Batch, 1968). Tryp-TAT shows low interaction with DNA compared to the other TAT peptides containing single hydrophobic residue at the N-terminal as seen from the zeta potential analysis. Tryptophan is the most hydrophilic amino acid amongst all the hydrophobic amino acids studied. Cationic vector/DNA complexes show a pronounced tendency to aggregate through Vander Waals and hydrophobic interactions when they are not highly charged (Erbacher, 1996). Tryptophan is known to intercalate between the base pairs of DNA (the interaction with DNA as seen from ethidium bromide assay is TAT ~ Tyr-TAT ~ Phe-TAT ~ Leu-TAT > Val-TAT > Tryp-TAT) (data not shown here).

Polyplexes formed from $Tyr_3$-TAT and $Tyr_5$-TAT have a relatively large size when compared to TAT or Tyr-TAT. The increase in zeta potential upon interaction of $Tyr_3$-TAT is more pronounced than Tyr-TAT and TAT (Fig. 2A). This indicates that $Tyr_3$-TAT modifies the surface characteristics of DNA while interacting moderately. This might be because of aggregation of the peptides and interaction of these aggregates with DNA. The cationic charges on $Tyr_3$-TAT would interact with the phosphate charges on DNA. However, the interaction of the hydrophobic domain of the peptide with the hydrophobic interior of DNA might be either reduced or prohibited because of the size of the hydrophobic domain. Therefore, these peptides might lie perpendicular to the surface of the DNA. The only way these hydrophobic domains could hide from the exterior aqueous environment is by aggregation.

Interaction of DNA with $Phe_3$-TAT and $Phe_5$-TAT indicates a slight increase in the zeta potential initially and upon further addition of the peptide, it becomes more negative and the size of the complexes formed indicates aggregation (Figs. 3B and 5). This phenomenon which, sometimes happens with lipid–DNA interaction, can be explained by the fact that as the DNA gets accumulated near the surface of peptide aggregates, the negative charge density increases. The hydrodynamic size that we see is a reflection of the size of aggregates of peptides and uneven distribution of the peptides and DNA. The low interaction might be because of more propensity of the peptide to aggregate. $Tyr_5$-TAT also behaves similarly because of the bulky hydrophobic domain that it has (Fig. 5).

Preliminary transfection studies indicated transfection efficiency that varied from 10 to 20% for hepatocytes HUH7 cells. Highest transfection efficiency was shown by the peptides containing more than 2 tyrosine residues on the N-terminal end of TAT–PTD. $Tyr_3$-TAT showed the highest transfection efficiency in hepatocyte HUH7 cells compared to its counterparts. A detailed evaluation of transfection efficiency and uptake characteristics needs to be done. A similar study done with Hel series peptides having a symmetrically varied hydrophobic–hydrophilic balance showed that the peptides with a large hydrophobic region took alpha helical structures and formed larger aggregates and also showed higher transfection efficiency. Their high efficiency was attributed to formation of stable aggregates which can be internalized by endocytosis and remain resistant to digestion in lysosomal vehicles (Ohmori et al., 1998).

Considering the size and electrokinetic properties of peptide–DNA complexes, we can classify the interaction of these peptides with DNA into two types (Fig. 5). Peptides having small hydrophobic area at N-terminal have a capacity to form smaller complexes depending on the nature of the hydrophobic domain, while peptides having larger hydrophobic tail at N-terminal have a tendency to aggregate forming larger complexes. However, the colloidal stability depends both on the nature of the hydrophobic domain as well as the type of complex formed.

## 4. Conclusion

The results obtained from gel electrophoresis, size and zeta potential analysis of TAT and modified TAT peptide–DNA complexes indicate that the presence of a hydrophobic domain at the N-terminal of the peptide does influence the complexation of the peptides with DNA. Peptides with smaller hydrophobic domain form smaller complexes and their stability in solution depends on the nature of the hydrophobic amino acid. The peptides with more than one hydrophobic aminoacid at N-terminal have a propensity towards aggregation and the resulting complexes can be either complexes of DNA–protein aggregates or an aggregate of DNA–peptide complexes.

## Acknowledgements

We thank Drs. Michael Bruist and Russel DiGate for their valuable suggestions during the course of this work. We thank Nucleonics Inc. for kindly donating the plasmid DNA and for their financial support of this project.

## References

Arnheiter, H., Haller, O., 1988. Antiviral sTATe against influenza virus neutralized by microinjection of antibodies to interferon-induced mdx proteins. EMBO J. 7, 1315–1320.

Blessing, T., Remy, J.S., Behr, J.P., 1998. Monomolecular collapse of plasmid DNA into stable virus-like particles. Proc. Natl. Acad. Sci. U.S.A. 95, 1427–1431.

Chakrabarti, R., Wylie, D.E., Schuster, S.M., 1989. Transfer of monoclonal antibodies into mammalian cells by electroporation. Biol. Chem. 264, 15494–15500.

Erbacher, P., 1996. Gene transfer by DNA/glycosylated polylysine complexes into human blood monocyte-derived macrophages. Hum. Gene Ther. 7, 721–729.

Fung, S.Y., Keyes, C., Duhamel, J., Chen, P., 2003. Concentration effect on the aggregation of a self-assembling oligopeptide. Biophys. J. 85, 537–548.

Gabbay, E.J., Kleinman, R.W., 1970. Topography of nucleic acid helices in solutions. The interaction specificities of optically active amino acid derivatives. Biochem. J. 117, 247–256.

Gottschalk, S., Sparrow, J.T., Hauer, J., Mims, M.P., Leland, F.E., Woosl, L., Smith, C., 1996. A novel DNA–peptide complex for efficient gene transfer and expression in mammalian cells. Gene Ther. 3, 448–457.

Gsponer, J., Haberthür, U., Caflisch, A., 2003. The role of side-chain interactions in the early steps of aggregation: molecular dynamics simulations of an amyloid-forming peptide from the yeast prion Sup35. Proc. Natl. Acad. Sci. U.S.A. 100, 5154–5159.

Ignatovich, I.A., Dizhe, E.B., Pavlotskaya, A.V., Akifiev, B.N., Burov, S.V., Orlov, S.V., Perevozchikov, A.P., 2003. Complexes of plasmid DNA with basic domain 47–57 of the HIV-1 TAT protein are transferred to mammalian cells by endocytosis-mediated pathways. J. Biol. Chem. 278, 42625–42636.

Kabanov, A.V., Astafieva, I.V., Chikindas, M.L., Rosenblat, G.F., Kiselev, V.I., Severin, E.S., Kabanov, V.A., 1991. DNA polyelectrolyte complexes as a tool for efficient cell transformation. Biopolymers 31, 1437–1443.

Kabanov, A.V., Kabanov, V.A., 1995. DNA complexes with polycations for the delivery of genetic material into cells. Bioconjug. Chem. 6, 7–20.

Keller, M., Tagawa, T., Preuss, M., Miller, A.D., 2002. Biophysical characterization of the DNA binding and condensing properties of adenoviral core peptide μ (mu). Biochemistry 41, 652–659.

Kyte, J., Doolittle, R.F., 1982. A simple method for displaying the hydropathic character of a protein. J. Mol. Biol. 157, 105–132.

Mahato, R.I., Monera, O.D., Smith, L.C., Rolland, A., 1999. Peptide-based gene delivery. Curr. Opin. Mol. Ther. 1, 226–243.

Malinin, V.V., Khavinson, V.K., 2005. Interaction between small peptides and DNA double helix. In: Gerontological Aspects of Genome Peptide Regulation. Karger, Basel, pp. 64–87.

Manickam, D.S., Bisht, H.S., Wan, L., Mao, G., Oupicky, D., 2005. Influence of TAT-peptide polymerization on properties and transfection activity of TAT/DNA polyplexes. J. Control. Release 102, 293–306.

Miller, R.I., Batch, D., 1968. Interaction of DNA with heavy metal ions and polybases: cooperative phenomenon. Biopolymers 6, 169–179.

Niidome, T., Ohmori, N., Ichinose, A., Wada, A., Mihara, H., Hirayama, T., Aoyagi, H., 1997. Binding of cationic a-helical peptides to plasmid DNA and their gene transfer abilities into cells. J. Biol. Chem. 272, 15307–15312.

Ohmori, N., Niidome, T., Kiyota, T., Lee, S., Sugihara, G., Wada, A., Hirayama, T., Aoyagi, H., 1998. Importance of hydrophobic region in amphiphilic structures of a-helical peptides for their gene transfer-ability into cells. Biochem. Biophys. Res. Commun. 245, 259–265.

Peggion, E., Verdini, A.S., Cosani, A., Scoffone, E., 1970. Conformational studies on polypeptides. Circular dichroism properties of random copolymers of lysine and phenylalanine in aqueous solutions at various pH values. Macromolecules 3, 194–197.

Rudolph, C., Planck, C., Lausier, J., Schillinger, U., Muller, R.H., Rosencker, J., 2003. Oligomers of the arginine-rich motif of the HIV TAT protein are capable of transferring plasmid DNA into cells. J. Biol. Chem. 278, 11411–11418.

Schwarze, S.R., Hruska, K.A., Dowdy, S.F., 2000. Protein transduction: unrestricted delivery into all cells? Trends Cell. Biol. 10, 290–295.

Sharma, V.K., Thomas, M., Klibanov, A.M., 2005. Mechanistic studies on aggregation of polyethylenimine–DNA complexes and its prevention. Biotechnol. Bioeng. 90, 614–620.

Sjögren, H., Ericsson, C.A., Evena, J., Ulvenlund, S., 2005. Interactions between charged polypeptides and nonionic surfactants. Biophys. J. 89, 4219–4233.

Sjögren, H., Ulvenlunda, S., 2005. Comparison of the helix–coil transition of a titrating polypeptide in aqueous solutions and at the air–water interface. Biophys. Chem. 116, 11–21.

Smith, L.C., Duguid, J.G., Wadhwa, M.S., Logan, M.J., Tung, C.H., Edwards, V., Sparrow, S.T., 1998. Synthetic peptide-based DNA complexes for non viral gene delivery. Adv. Drug Deliv. Rev. 30, 115–131.

Straubinger, R.M., Duzgunes, N., Papahadjopoulos, D., 1985. pH sensitive liposomes mediate cytoplasmic delivery of encapsulated macromolecules. FEBS Lett. 179, 148–154.

Vijayanathan, V., Thomas, T., Shirahata, A., Thomas, T.J., 2001. DNA condensation by polyamines: a laser light scattering study of structural effects. Biochemistry 40, 13644–13651.

Wadhwa, M.S., Collard, W.T., Adami, R.C., Mckenzie, D.L., Rice, K.G., 1997. Peptide mediated gene delivery influence of peptide structure on gene expression. Bioconjug. Chem. 8, 81–88.

Yoshikawa, Y., Yoshikawa, K., 1995. Diaminoalkanes with an odd number of carbon atoms induce compaction of a single double-stranded DNA chain. FEBS Lett. 361, 277–281.